Proceedings of the 9ICEG
9th International Congress on Environmental Geotechnics
25-28 June, 2023 | Chania, Greece
© Authors: All rights reserved, 2023
https://doi.org/10.53243/ICEG2023-240

Predicting the Longevity of Permeable Reactive Barriers Installed in Acid Sulfate Soils

Subhani Medawela[1], and Buddhima Indraratna[2]

[1]*Research Fellow, Faculty of Engineering and Information Technology, University of Technology Sydney, Australia, email: subhani.medawela@uts.edu.au*

[2]*Director, Transport Research Centre (UTS-TRC), Faculty of Engineering and Information Technology, University of Technology Sydney, Australia, email: buddhima.indraratna@uts.edu.au*

ABSTRACT

Column experiments were conducted to evaluate the potential use of calcitic limestone as a reactive material in permeable reactive barriers (PRBs) and its clogging behaviour in the presence of continuous acidic flow containing Al, Fe, and acidophilic bacteria. The findings revealed that the biogeochemical clogging in the column was not consistent along the flow path, with the ability to neutralise the acid at the inlet zone losing effectiveness after 75 days, whereas the acid neutralisation at the outlet remained satisfactory throughout 245 days. Additionally, a numerical model was employed to estimate the longevity of the limestone assembly in regards to neutralising acid and removing excessive concentrations of metals. This model incorporates the governing equations for contaminant transport through porous media and the biogeochemical reactions between the acidic input and the alkaline PRB media using MODFLOW and RT3D software codes. The model predictions aligned with the laboratory findings and affirmed that the chosen calcitic limestone batch, which has a 97% $CaCO_3$ composition, is appropriate to serve as a reactive material in a PRB installed in an acid sulfate soil site in NSW, Australia. The lifespan predicted by the numerical model for this PRB is approximately 16 years.

Keywords: Acid Sulfate Soil, Groundwater, Permeable Reactive Barriers, Bio-geochemical Clogging

1 INTRODUCTION

The impacts of acid sulfate soil on the environment and ecology have been intensified by climate change and recent extreme weather conditions in Australia and many coastal regions worldwide (Fitzpatrick et al., 2011). During periods of drought or excavation for construction and mining, if the water table is lowered, shallow deposits of pyrite (FeS_2) can be uncovered to the air and rapidly oxidise, leading to the production of sulfuric acid and soil and groundwater contamination (Shand et al., 2018). In acidic environments, metals like aluminium (Al) and iron (Fe) can be released from the soil and readily dissolve in groundwater, affecting estuarine ecosystems and retarding plant growth, causing fish diseases and hindering agricultural and aquaculture development. Acidic groundwater also has a highly corrosive effect on steel and concrete infrastructure (Högfors-Rönnholm et al., 2018; Medawela et al., 2019). In Australia, over 3 million hectares of coastal land are covered by acid sulfate soil, and the yearly damage caused by acidic soil and water is projected to cost millions of dollars (EPHC, 2011). Therefore, remediation of contaminated water in acidic floodplains is a critical need. The method of treatment for acidic soil and groundwater depends on the specific characteristics of each aquatic ecosystem, such as the type and concentration of contaminants, the discharge volume, the quality standards set by regulatory agencies, and the intended use of the treated water.

Permeable reactive barriers (PRBs), which are zones of reactive granular materials placed underground, are a cost-effective way to neutralise acidic groundwater when filled with alkaline aggregates (Gavaskar et al., 2005). Ongoing monitoring of the flow through PRBs installed in the Shoalhaven acidic floodplain, NSW, Australia, over the past 16 years has verified that they are able to effectively decontaminate the acidic inflow (Indraratna et al., 2014; Medawela et al., 2022). The interaction between acidic groundwater and alkaline media can form chemical precipitates covering the surfaces of aggregates, known as chemical armouring. These secondary mineral precipitates also

cause blockage of the pores in the granular matrix, referred to as geochemical clogging. Furthermore, groundwater also carries bacteria living in pyritic soils into the PRB. These microbes grow in the pores and surfaces of the reactive materials, leading to biological clogging. For instance, *Acidithiobacillus ferrooxidans*, a commonly found iron-oxidising bacteria (IOB) in acidic environments, can catalyse the oxidation of Fe^{2+} to Fe^{3+}, accelerating the formation of iron precipitates. The filling of a large portion of the pore volume with biomass and chemical precipitates results in a significant reduction in the porosity of the granular filter (PRB), which affects the effectiveness of acid neutralisation and metal removal (Medawela et al., 2023). Therefore, it is crucial to evaluate the coupled clogging to maintain optimal PRB performance. This paper outlines experiments and a numerical approach that can be used to analyse the biogeochemical clogging of a PRB installed in an acid sulfate soil terrain.

2 METHODOLOGY

According to the Australian water quality guidelines, water should have a pH between 6.5 and 8.5 for the well-being of plants and animals and to avoid corrosion and scaling of pipes and fittings (NRMMC 2011). The standard levels of Al and Fe in water should be below 0.5 mg/L (ANZECC, 2000). Despite this, monitoring of the groundwater in the Shoalhaven floodplain, 130 km south of Sydney, NSW, Australia, over the past 16 years has revealed it to be highly acidic (pH around 3.5) with high levels of aluminium (54 mg/L) and iron (91 mg/L) (Golab et al. 2006, Indraratna et al. 2010, 2020). Thus, a pilot-scale PRB made of limestone aggregates was installed to neutralise the acidity of groundwater and reduce high levels of Al and Fe. The PRB measures 18 m in length, 3 m in depth, and 1.2 m in width, with the groundwater flowing through the width (1.2 m). Before implementing a PRB in the field, it is crucial to evaluate the effectiveness of the chosen material in neutralising acid and removing other target contaminants from groundwater through laboratory testing. Also, during the design stage of a real-life PRB, it is essential to predict its long-term performance using an appropriate numerical approach.

The limestone particles (consisting of 97% calcium carbonate) used in the PRB were obtained from a quarry in Moss Vale, Australia. Aggregates from the same batch were tested in column experiments to determine if they could effectively remove acidity and metals to meet regulatory standards. A comprehensive explanation of the experimental process is provided by Indraratna et al. (2020), while only a brief overview of the technique used to evaluate clogging in laboratory columns is outlined below.

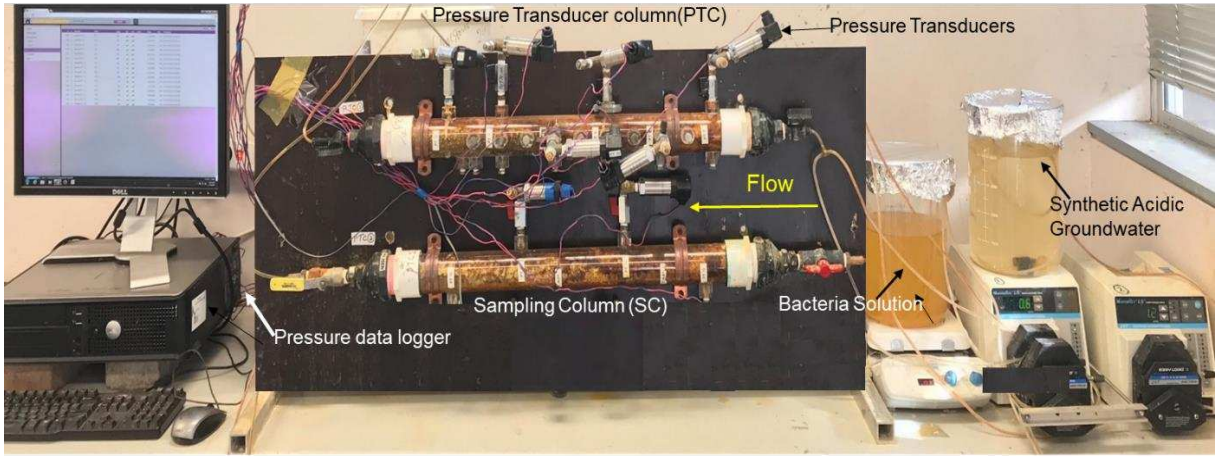

Figure 1. *Laboratory column test setup*

The experimental setup consisted of two acrylic tubes (Figure 1): the sample column (SC) and the pressure transducer column (PTC). Both columns were of the same length (650 mm) and diameter (50 mm) and filled with limestone aggregates with a median particle size of 5 mm. Synthetic groundwater was pumped through the columns at a rate of 1.2 ml/min to simulate the levels of contaminants present in the groundwater of the Shoalhaven acidic floodplain (pH = 3.5, [Al]= 54 mg/L, [Fe]= 91 mg/L). The flow direction was assumed to be horizontal. The initial volume of voids of SC and PTC, referred to as pore volume (PV) in this paper, were 682 ml and 672 ml, respectively. A multi-parameter water quality meter was used to measure the pH of the specimens collected from the sampling column (SC). The concentrations of Fe and Al in the specimens were assessed using inductively coupled plasma optical emission spectroscopy. Water samples were not taken from the PTC to minimise the disturbances on pressure readings, and it was solely used to measure changes in the porewater pressure. The

experiment also aimed to imitate the potential growth of bacteria in the limestone media. This was done by introducing a culture of iron oxidising bacteria (*Acidithiobacillus ferrooxidans*), which is commonly found in the Shoalhaven floodplain, into the columns. This strain of bacteria grows optimally at a pH of 2-2.5 (Rawlings, 2002). Therefore, the suspension of bacteria was added to the flow when the pH at the inlet of the column fell below 4.5. The changes in bacterial cell density were monitored by analysing water samples from the column using a Helber counting grid and an optical microscope.

The experiment was concluded when the pH of the effluent dropped below the influent pH after a total of 790 PVs (260 days). The columns were allowed to air dry for two weeks, and samples were taken from the inlet (0 to 0.15 m length), middle (0.15 m to 0.35 m), and outlet (0.35 m to 0.5 m) zones of the column. A portion of the aggregates extracted from each zone was repeatedly rinsed with distilled water and passed through a filter paper with a pore size of 0.45 µm until it became clear. The residues on the filter paper, i.e. mineral coating extracted from aggregates, were oven-dried. The remaining aggregates that were not rinsed were ground into a fine powder. Then X-ray diffraction was performed on these samples using a GBC MMA XRD machine, and the analysis was conducted using X'Pert HighScore software. Additionally, each sample was examined through scanning electron microscopy (SEM) and energy-dispersive X-ray spectroscopy (EDS) to assess the extent of clogging in each region.

3 RESULTS AND DISCUSSION

3.1 Removal of acid by limestone

In comparison to the low pH of the influent water (pH~3.5), the pH of the water flowing through the column was significantly increased and reached the standard limit at the outlet [Figure 2(a)]. At the start of the test, the pH of the column discharge reached 8, which may have been caused by the rapid dissolution of $CaCO_3$ from the limestone upon being exposed to the acidic flow. Afterwards, the pH of the water stayed close to neutral (pH ~ 6.5) from 80 PV to 190 PV. This result could be due to the bicarbonate buffering of limestone, which occurs when HCO^{3-} ions are released (Table 1).

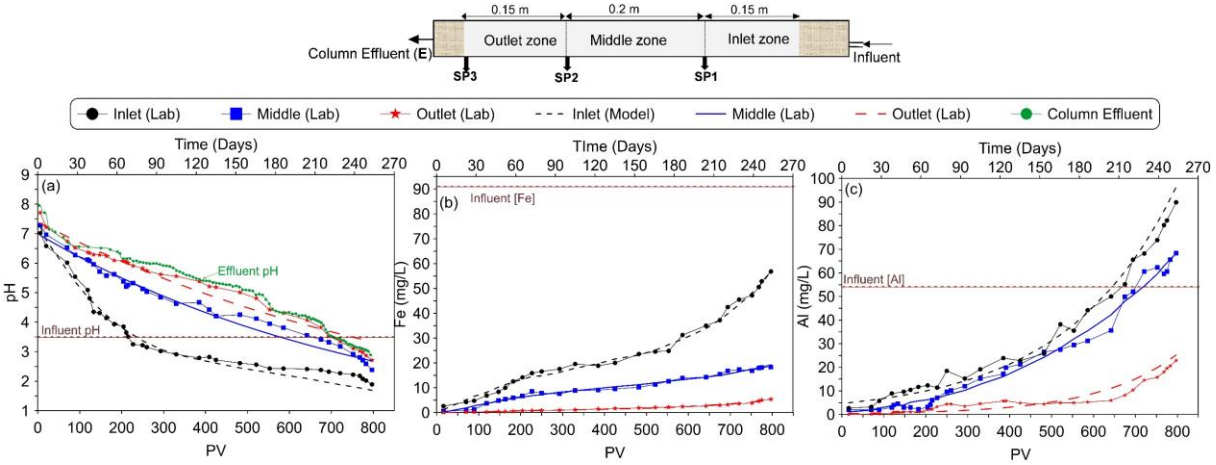

Figure 2. *Removal of acidity and metals from limestone (a) pH (b) Fe (C) Al (Data sources: Indraratna et al. 2020, Medawela, 2020)*

During the interval from 80 PV to 190 PV, the amount of Al and Fe in the water that flowed out of the column was significantly lower than the amount in the incoming water [Figures 2(b) & 2(c)]. The decrease in Al and Fe levels implies that these ions were captured by the alkaline granular matrix as mineral deposits, according to the reactions shown in Table 1. This suggests that bicarbonate buffering is the crucial phase of treatment by limestone, as it effectively removes the designated pollutants, acidity, and high levels of metals.

After 190 PV, the pH of the column discharge gradually declined and reached 4.81 at 550 PV and then abruptly dropped, likely due to the depletion of alkalinity in the aggregates after prolonged exposure to acidic water. The concentration of dissolved Al in the effluent started to increase shortly after the pH at the outlet dropped below 4 at 670 PV, reaching 20 mg/L by the end of the test [Figure 2(c)]. This is because pH ~4 is the buffering point at which Al precipitates redissolve. After prolonged exposure to

acidic water, the redissolution of Al oxides and hydroxides could no longer effectively buffer the acidity. Ferric hydroxides maintain a pH of around 3.5 when close to equilibrium (Johnson et al. 2000), but the quantity of Fe precipitates was insufficient to sustain the pH for an extended period. As a result, the pH of the column effluent eventually reached the same level as the influent after 700 PV. In the final stages, the increase in dissolved Al and Fe concentrations in samples taken from the column suggests that these ions were no longer retained within the granular structure, which could have occurred due to its armouring and clogging.

Table 1. *Chemical and biological reactions between limestone and acidic water (Source: Medawela & Indraratna (2020))*

Description	Dissolution/Precipitation Reaction	Kinetic rate coefficients (k) $molL^{-1}s^{-1}$	
		Laboratory	Field
Limestone dissolution	$CaCO_3 + 2H^+ \leftrightarrow Ca^+ + H_2CO_3$	2.43E−07	7.21E−08
	$CaCO_3 + H_2CO_3 \leftrightarrow Ca^{2+} + 2HCO_3^-$	2.43E−07	7.21E−08
Ferrous oxidation - chemical	$Fe^{2+}_{(aq)} + 1/4\, O_{2(aq)} + H^+_{(aq)} \rightarrow Fe^{3+}_{(aq)} + 1/2\, H_2O$	5.62E−08	1.97E−08
Ferrous oxidation – by bacteria	$Fe^{2+}_{(aq)} + 1/4\, O_{2(aq)} + H^+_{(aq)} \xrightarrow{IOB} Fe^{3+}_{(aq)} + 1/2\, H_2O$	3.09E−07	9.82E−08
Formation of mineral precipitates	$Fe^{3+} + 3H_2O \rightarrow Fe(OH)_{3(s)} + 3H^+_{(aq)}$	8.98E−08	2.81E−08
	$Fe^{3+} + 2H_2O \rightarrow Fe(OOH) + 3H^+_{(aq)}$	8.49E−08	2.56E−08
	$2Fe^{3+} + 3H_2O \rightarrow Fe_2O_3 + 6H^+_{(aq)}$	7.81E−08	2.62E−08
	$Al^{3+} + 3H_2O \rightarrow Al(OH)_{3(s)} + 3H^+_{(aq)}$	3.03E−07	8.98E−08

The effectiveness of neutralising the acidity of groundwater and removing metals varied in each section of the columns. For instance, the pH at the inlet rapidly dropped to the acidity of the incoming water (pH = 3.5) after 230 PVs (78 days), while the middle and outlet sections took longer, i.e. 630 PV (215 days) and 720 PVs (245 days), respectively. This is because the inlet zone partially neutralises the highly acidic groundwater as soon as it reacts with limestone aggregates in the first 0.15 m of the column. Then the second zone (0.15 m – 0.25 m) exposes to lesser acidity than the inlet zone; therefore, the armouring in this middle zone is lesser than the inlet. Subsequently, the outlet zone is exposed to the least acidic groundwater, causing minimum armouring and hence preserving the reactivity of the aggregates in this area longer. These findings are further supported by the mineralogical analysis of the coated aggregates from different sections, discussed in the next section.

3.2 Mineralogical analysis of armoured aggregates

Table 2 summarises the X-ray diffraction analysis of minerals based on weight percentages. It displays the mineral composition of the limestone aggregates before being used in the experiment, the aggregates with surface armouring, and the mineral coating extracted from various regions of the columns.

Table 2. *The mass percentage of various mineral phases in fresh limestone, armoured limestone, and the mineral coating extracted from armoured aggregates (Source: Medawela et al., 2023)*

Mineral Phase	Percentage by weight (%)								
	Inlet zone(0 – 0.15m)			Middle zone			Outlet zone		
	FL[1]	AA[2]	MC[3]	FL[1]	AA[2]	MC[3]	FL[1]	AA[2]	MC[3]
Calcite ($CaCO_3$)	97.1	71.6	17.1	97.1	79.2	22.8	97.1	89.2	36.4
Dolomite ($CaMg(CO_3)_2$)	1.1	0.3	0.3	1.1	0.4	0.4	1.1	0.4	0.5
Hematite(Fe_2O_3)	0.1	8.2	28.3	0.1	5.4	22.6	0.1	4.3	16.5
Goethite (FeOOH)	0	10.8	31.2	0	8.5	27.8	0	3.2	19.4
Alumina (Al_2O_3)	0.2	3.3	11.2	0.2	1.6	12.9	0.2	1.4	10.9
Boehmite (AlOOH)	0.3	5.8	11.9	0.3	4.9	13.5	0.3	1.5	16.3

[1] FL = Fresh Limestone , [2] AA = Armoured aggregates, [3]MC = Extracted mineral coating

The data demonstrates that the limestone originally consisted of 97.1% calcite and 1.1% dolomite; however, due to the continued dissolution of Ca minerals in acidic water, the amount of $CaCO_3$ in the coated limestone has decreased. The presence of Hematite (Fe_2O_3), Goethite (FeOOH), Alumina

(Al_2O_3), and Boehmite (AlOOH) in the aggregates was negligible before starting the column test. The rise in these Al and Fe-bearing mineral percentages in coated aggregates demonstrates the formation of precipitates on the aggregate surface. The XRD analysis also confirmed that the clogging and armouring were uneven in three adjacent zones of the column. At the end of the experiments, the quantity of calcite had decreased by 26.2% at the inlet, 18.4% in the middle, and 8.1% at the outlet. The calcite decrease was less at the outlet, meaning the depletion of alkalinity was also less at the outlet. The highest concentration of Fe and Al minerals in the armoured aggregates was found in the inlet, with the lowest concentration at the outlet. The reduction in weight of Hematite (Fe_2O_3), Goethite (FeOOH), Al_2O_3, and AlOOH from the inlet to the outlet was over 50%.

Based on the results from SEM-EDS analysis, the amount of calcium in fresh limestone was found to be higher, as indicated by the higher calcium peak in the EDS plot [Figure 3(a)], compared to the armoured aggregates, as seen in the much lower calcium peaks in Figures 3 (b, c, & d). On the other hand, Fe and Al peaks were barely present in the fresh limestone but were clearly visible on the coated particles from the inlet at the column, indicating the presence of precipitates. The SEM images of the fresh particles in Figure 3(a) only show the limestone surface, while the images of the samples from the inlet show that it has encrusted making it difficult to see any limestone aggregates [Figure 3(b)]. The highest peaks for Fe and Al in EDS graphs were found at the inlet [Figure 3(b)], suggesting an increased amount of encrustation at the entrance compared to the middle [Figure 3(c)] and the outlet [Figure 3(d)]. As the peaks representing Ca increased along the column while those representing Fe and Al decreased, these observations infer that the degree of clogging and armouring decreased along the column.

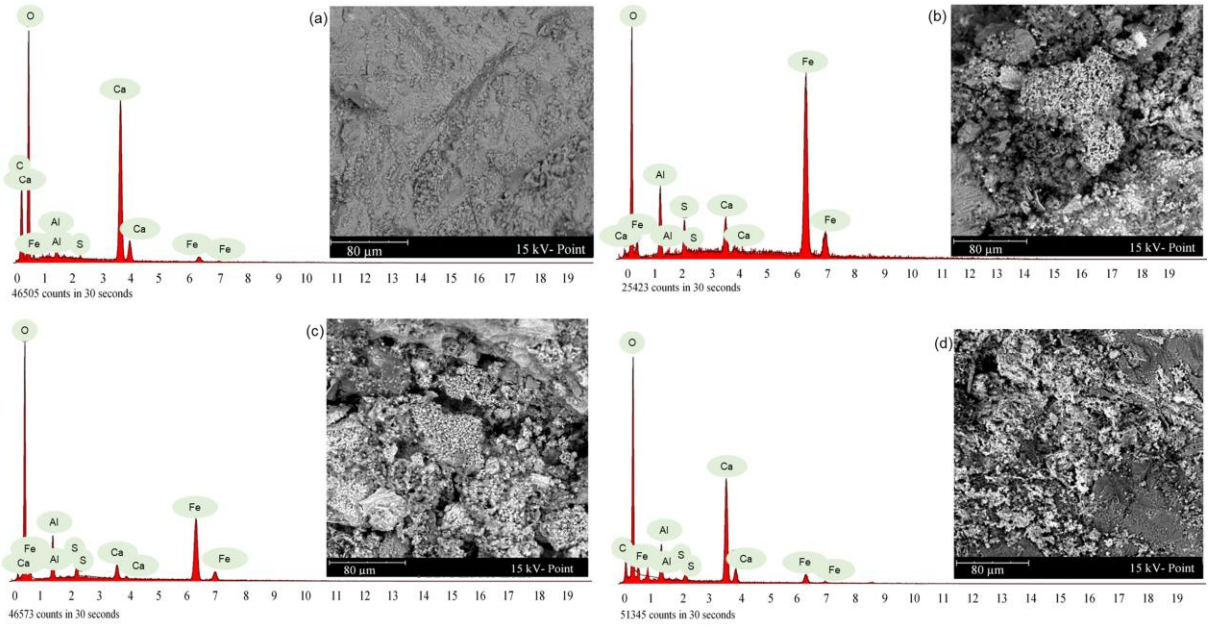

***Figure 3**. Energy-dispersive X-ray spectroscopy (EDS) analysis of limestone: (a) Fresh limestone, Armoured aggregates from (b) inlet (c) middle zone (d) outlet (Modified after Indtraratna et al. 2020)*

4 MODELLING THE CLOGGING OF GRANULAR BARRIER

Table 3 summarises the equations used to solve the one-dimensional form of the fundamental equation that governs fluid flow through porous materials. The hydraulic head, h(x,t), at a certain time (t) and location (x) along the direction of groundwater flow is captured by this solution, taking biogeochemical clogging of the porous media into account. Medawela and Indraratna (2020) employed a combination of commercially available groundwater modelling software, MODFLOW and RT3D, to develop a model for predicting fluid flow and reactive contaminant transport through limestone columns and the PRB installed in the Shoalhaven floodplain. The set of chemical and biological reactions that occur in a granular limestone assembly when exposed to acidic groundwater (see Table 1) were integrated into the model using FORTRAN subroutines. The equations listed in Table 3 were utilised to generate input data arrays that account for the changing porosity and hydraulic conductivity over time.

Table 3. *Equations used in the biogeochemical reactive transport model (Source: Indraratna et al. 2020, Medawela & Indraratna 2020)*

Parameter		Equation	Definition of terms
Time-dependent porosity	Porosity reduction due to biological clogging	$\Delta n_{t_{(bio)}} = \frac{X_0 e^{k_c t}}{\rho_c \left(1 - \frac{X_0}{X_\infty}(1 - e^{k_c t})\right)}$ (Monod, 1949)	X_0 = initial concentration of bacterial cells observed in influent [ML^{-3}] X_∞ = maximum concentration of bacterial cells in the granular assembly [ML^{-3}] X_t = bacterial cell concentration [ML^{-3}] at time *t* [T] k_c = carrying capacity coefficient [T^{-1}] ρ_c = solid phase biomass density [ML^{-3}] M_k = molar volume of minerals (m^{3}mol^{-1}) $R_k = \sum_{i=1}^{N} r_i$ = overall reaction rates for Ca, Fe or Al minerals (molm^{-3}s^{-1}) $r_i = -k\left(1 - \frac{IAP}{K_{eq}}\right)$ = reaction rate of each precipitation or dissolution reaction (molm^{-3}s^{-1}) *k* = kinetic rate coefficient (molm^{-3}s^{-1}) for each reaction (see Table 1) IAP = iron activity product K_{eq} = equilibrium coefficient
	Porosity reduction due to chemical clogging	$= \sum_{k=1}^{m} M_k R_k t$ (Steefel & Lasaga, 1994)	
	Total reduction in porosity	$\Delta n_t = \Delta n_{t_{(bio)}} + \Delta n_{t_{(che)}}$	
	Porosity at time t	$n_t = n_0 - \Delta n_t$	
Hydraulic Conductivity		$K = K_0 \left[\frac{n_0 - \Delta n_t}{n_0}\right]^3 / \left[\frac{1 - n_0 + \Delta n_t}{1 - n_0}\right]^2$	K = timely varied hydraulic conductivity [LT^{-1}] K_o = Initial hydraulic conductivity [LT^{-1}]
Transient flow through a porous media		$\frac{\partial}{\partial x}\left(K_{xx}\frac{\partial h}{\partial x}\right) + \frac{\partial}{\partial y}\left(K_{yy}\frac{\partial h}{\partial x}\right) + \frac{\partial}{\partial z}\left(K_{zz}\frac{\partial h}{\partial z}\right) + W = S_s\frac{\partial h}{\partial t}$ (Harbaugh, 2005)	K_{xx}, K_{yy}, K_{zz} = hydraulic conductivity along the *x*, *y*, and *z* coordinate axes *h* = hydraulic head (L) *W* = volumetric flux per unit volume representing sources and/or sinks of water S_s =specific storage of the porous material (L^{-1})
Solution for the one-dimensional formulation of flow equation		$h(x,t) = F(x).e^{F(t)}$ (Indraratna et al., 2020)	$F(x) = (C_1 sinCx + C_2 cosCx)$; C, C$_1$,C$_2$ = Integral constants $F(t) = \frac{-C^2}{B}\left(-\frac{\sum_{k=1}^{N_m} M_k R_k t^2}{2} + \frac{X_\infty}{\rho_c K_c} ln\left[1 - \frac{X_0}{X_\infty}(1 - e^{k_c t})\right] + (n_o + 2)t - 3ln[\Delta n_t - n_o + 1] + 3ln\left[\frac{X_0}{\rho_c} - n_o + 1\right] + \frac{1}{\Delta n_t - n_o + 1} - \frac{1}{\left(\frac{X_0}{\rho_c} - n_o + 1\right)}\right)$ (Indraratna et al., 2020)

The model outputs, including variations of ion concentrations and pH along the reactive granular assembly, were used to assess the longevity of the PRB.

4.1 Applying model to the column experiments

The simulation of flow through laboratory columns using the model was based on the assumption that a column represents a confined, uniform, and isotropic aquifer with relatively consistent particle angularity throughout and experiences transient flow conditions. It was also assumed that the flow within the column was mainly horizontal, resulting in limited lateral and vertical flow in the limestone aquifer. The model used a single-layer grid to represent the one-dimensional flow through a layer of uniform thickness along the centerline of a 500 mm long and 50 mm wide column [Figures 4(a)]. The domain was evenly divided into 5 x 50 grid cells, each measuring 10 mm in length and 10 mm in width. The inlet and outlet were initially considered to be fixed head boundaries, and the sides of the column were considered to be no-flow boundaries. The flow was introduced by specifying wells with a positive flow rate at the inlet. Model input parameters are given in Table 4.

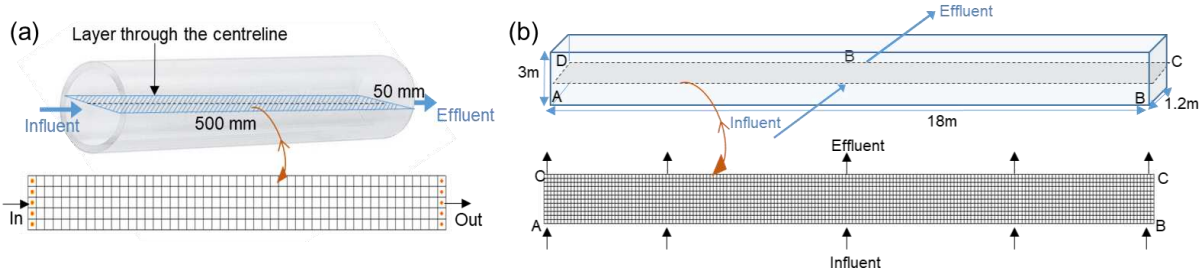

Figure 4. *Model domains (a) limestone column (b) field PRB (Modified after Medawela, 2020)*

Table 4: *Input parameters for bio-geochemical transport model (Source: Medawela, 2020)*

Input parameter	Lab Columns	Field PRB
Dimensions	0.05 m X 0.5 m	18 m x 3 m x 1.2 m
Flow rate	1.2 mL/min	1.1 x 10^6 L/ year
Porosity of the aquifer *(n_0)*	0.68	0.69
Hydraulic conductivity of the aquifer *(K_0)*	1·8 ×10^{-5} m/s	0.9565 m/day
Influent pH	3.5	3.7
Ca of influent	152 mg/L	152 mg/L
Fe of influent	91 mg/L	91 mg/L
Al of influent	54 mg/L	54 mg/L
Bacteria Concentration of influent	10^7 cells/ cm^3	10^7 cells/ cm^3
Initial [Ca^{2+}]	620 mg/L	700
Initial concentrations within the aquifer: [Fe], [Al]	0	0
Initial cell density of bacteria in the aquifer	0	0

The model predictions and the measured pH values at the inlet, middle, and outlet regions of the column were found to be in agreement, particularly during the first half of the experiment [see Figure 2]. However, some minor differences emerged during the final stages of the experiment, which arose from the use of the maximum kinetic rate (*k* in Table 1) throughout the length of the column. The rate coefficients for each biochemical reaction within the reactive granular assembly were initially estimated. Then these unknown parameters were refined to ensure that the modelled hydraulic head [h(x,t) from Table 3] matched the hydraulic head determined from piezometer readings obtained from PTC (Indraratna et al., 2020). However, determining the spatial and temporal variations of multiple kinetic rate coefficients (k_{CaCO3}, $k_{Al(OH)3}$, $k_{Fe(OH)3}$, k_{FeOOH},k_{Fe2O3}) for the inlet, middle, and outlet regions of the column over 800 PVs using a trial and error approach is time-consuming. Therefore, these values were only determined for the inlet region, where the highest level of clogging occurs due to biologically-driven mineral precipitation, while the fouling in subsequent regions is less significant, as discussed in Section 3.1. Therefore, the kinetic rate coefficients for the inlet region were applied to the entire length of the column, despite the fact that in reality, the kinetic rate coefficients should be lower in the middle and outlet regions. This results in the model slightly overestimating clogging in the outlet, leading to lower predicted pH values than the actual values. However, using the maximum rate kinetics throughout the

entire length is a conservative approach as it predicts the earliest possible time when the hydraulic head, and thus the hydraulic conductivity within the granular assembly, would drop below a specific limit. Additionally, the model accurately predicted the removal of target ions [see Figures 2(b) & (c)] and showed that these ion levels at the outlet met the standards until the pH of the discharge began to drop below 6.5.

4.2 Applying the model to a field PRB

The biochemical reactions that take place in column experiments and a real-life PRB are the same. However, groundwater treatment tends to occur in an accelerated manner in laboratory simulations due to strict control over conditions such as constant pH, specific concentrations of Al, Fe, and IOB in the inflow, fixed flow rates, smaller particle sizes, and constant temperature. As a result, incorrect results may be obtained if the laboratory-based reaction kinetics which may differ from natural systems, are used to model biogeochemical clogging in a field PRB. Hence, it is critical to scale up the reaction rates derived from laboratory observations to the field scale when designing a real-life PRB. Thus the upscaled rate kinetics from the laboratory scale to the field scale based on dimensional analysis (see Table 1) were used in the model to predict the longevity of the PRB installed in the Shoalhaven floodplain. The reaction kinetics found in laboratory experiments are higher than that calculated for the field scale by a minimum of three times (Medawela & Indraratna, 2020).

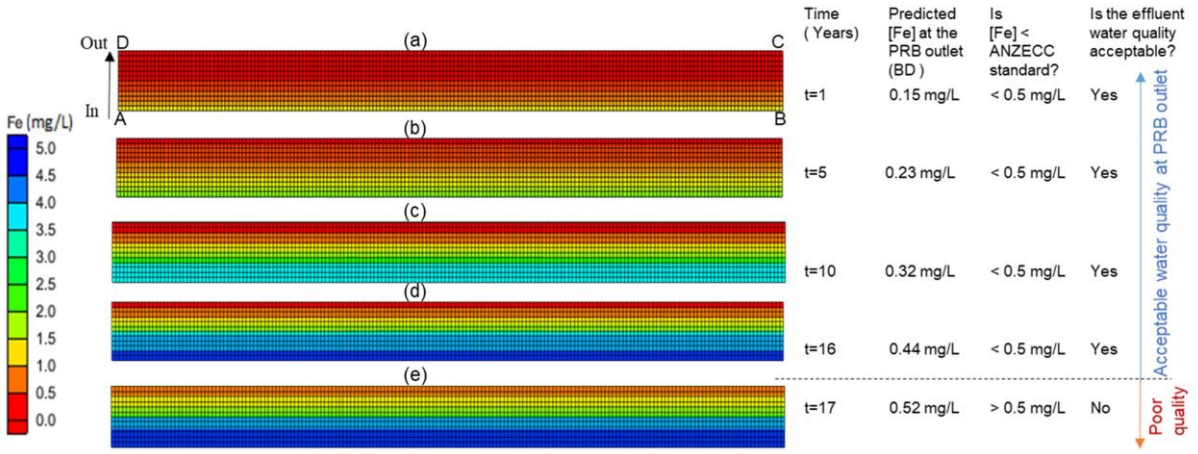

Figure 5. *Model predictions for the variation of [Fe] along the centreline of the PRB (modified after Medawela, 2020)*

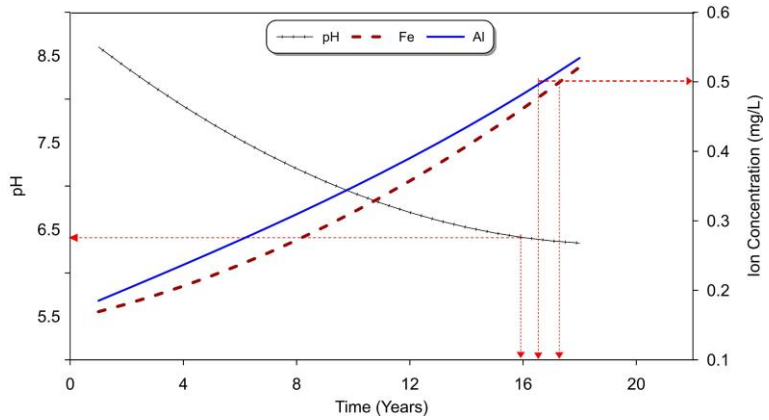

Figure 6. *Model predictions on pH and ions at the PRB outlet (Modified after: Medawela et al., 2023)*

The model simulated one-dimensional flow along the centerline of the PRB to investigate the elimination of acidity and metals from groundwater as it flows through porous limestone over 20 years. The porous media was assumed to be a homogeneous and isotropic aquifer comprised of limestone aggregates with a near-uniform size (d_{50} = 40 mm) and a uniformity coefficient of 1.8, having a similar particle angularity. The PRB can be divided into several hypothetical horizontal layers along its depth (as shown in Figure 4(b), labelled as the ABCD layer), which coincides with the centerline of the PRB. The ABCD layer has a uniform thickness and represents a 1.2 m x 18 m layer model domain with 12 x 180 grid

cells. If it is assumed that vertical and lateral flows are negligible, the horizontal flow through each column of the ABCD layer can be analysed. By stacking multiple ABCD layers of unit thickness on top of each other from the top to the bottom of the PRB, the horizontal flow through its entire depth can be modelled.

The concentration of Fe in the ABCD layer of the PRB is displayed in Figures 5 (a) to 5(e), showcasing its changes over 17 years. The simulation projects that the iron concentration at the outlet (CD side) of the PRB would reach 0.15 mg/L at the end of the first year [Figure 5(a)] but then rise to 0.44 mg/L within 16 years [Figure 5(d)]. By the 17th year, the expected concentration of Fe at the outlet surpasses 0.5 mg/L [Figure 5(e)], the maximum limit established by the ANZECC (2000) guidelines for Fe in water sources. This indicates that the efficiency of the limestone granular assembly in producing iron-free water decreases after 16 years. In the same way, the variations in the concentrations of other target pollutants, Al and pH, can be estimated. As illustrated in Figure 6, the simulation predicts that by the 17th year of operation, the expected Al level at the outlet would increase to 0.57 mg/L, which exceeds the acceptable limit. This implies that the discharge from the PRB is anticipated to be free of Al and Fe for the first 16 years. The simulation results also suggest that the starting pH of the discharge would increase to 8.67, then gradually decrease to 6.75 within 16 years. However, after 17 years, the pH at the outlet is expected to become acidic (Figure 6). Therefore, it can be inferred that the PRB is expected to generate nearly neutral effluent for the first 16 years. To summarise, this PRB is estimated to have effective longevity of approximately 16 years to neutralise acid and remove toxic metals, after which the water quality of the effluent will deteriorate.

4 CONCLUSIONS

Experiments and numerical simulations were performed to evaluate the treatment capacity of a pilot-scale PRB located in a low-lying pyritic floodplain in Shoalhaven, NSW, Australia. In order to create more realistic field conditions in the laboratory, synthetic acidic groundwater was used that mimicked the water chemistry and iron oxidising bacteria levels at the PRB site. The results led to the following conclusions.

The results showed that using limestone aggregates to treat acidic groundwater in the Shoalhaven floodplain was effective. The most efficient treatment occurred during the bicarbonate buffering phase of the column experiments, which was found to occur within a quarter of the total test duration. The biogeochemical reactive transport model estimated that the optimum treatment of an actual pilot-scale PRB in the area would occur within the first 16 years of operation. However, the model also indicated that the alkalinity of the limestone media would eventually be depleted. Thus, it is essential to identify the duration of bicarbonate buffering for a PRB through model simulations to determine its longevity.

The results showed that the armouring and biogeochemical clogging were not evenly distributed throughout the flow path of the groundwater, with the highest intensity at the inlet and becoming less intense towards the outlet of the granular assembly. The pH increase at the inlet of the column was initially successful but rapidly dropped to the influent pH level after only 2.5 months, even before the experiment was half over. On the other hand, the acid neutralisation at the outlet was adequate for about 8 months before the acidity increased again. Therefore, despite the severe clogging and failure of acid neutralisation at the inlet of a PRB, the outlet can still generate an effluent of the required quality for a long time.

It is crucial to consider the scaling of reaction rates when using the biogeochemical reactive transport model to predict the performance of a PRB in the field. In this study, it was found that laboratory-scale reaction rates were almost three times higher than the field-scale reaction rates, highlighting the importance of using accurate kinetic rates to avoid incorrect predictions.

ACKNOWLEDGEMENTS

The authors are grateful for the funding received from the Australian Research Council (ARC) and the industry partners, Manildra Group-Shoalhaven Starches, Glencore Pty Ltd and Douglas Partners Pty Ltd. The efforts of UTS technical staff are kindly acknowledged.

REFERENCES

ANZECC (Australian and New Zealand Environment Conservation Council), 2000. Australian and New Zealand Guidelines for Fresh and Marine Water Quality. Australian and New Zealand Environment and Conservation Council and Agriculture and Resource Management Council of Australia and New Zealand, Canberra, pp. 1–103.

Environmental Protection and Heritage Council (EHPC), 2011. National Guidance on Acid Sulphate Soils, ISBN 978-1-921733-09-3.

Gavaskar, A, Yoon, W, Sminchak, J, Sass, B, Gupta, N, Hicks, J & Lal, V 2005, Long Term Performance Assessment of a Permeable Reactive Barrier at Former Naval AITR Station Moffett Field, (No. NAVFAC-CR-05-006-ENV), *DTIC Document. Available at < https://apps.dtic.mil/dtic/tr/fulltext/u2/a446918.pdf>*

Gillham, RW & O'Hannesin, SF 1994, 'Enhanced degradation of halogenated aliphatics by zero-valent iron', *groundwater*, vol. 32, no. 6, pp. 958-67.

Golab AN, Indraratna B, Peterson MA & Hay S. 2006. Design of a permeable reactive barrier to remediate acidic groundwater. *ASEG Extended Abstracts,* 2006**,** 1-3(*DOI*: https://doi.org/10.1071/ASEG2006ab051).

Fitzpatrick R, Shand P & Hicks W. 2011. Technical guidelines for assessment and management of inland freshwater areas impacted by acid sulfate soils. *CSIRO Land and Water Science Report,* 5**,** 160. https://doi.org/10.5072/83/5849a13e94e13

Harbaugh, AW 2005, *MODFLOW-2005, the US Geological Survey modular groundwater model: the groundwater flow process*, US Department of the Interior, USGeological Survey Reston, VA, USA.

Högfors-Rönnholm E, Christel S, Dalhem K, lillhonga ., Engblom S, Österholm P & Dopson M. 2018. Chemical and microbiological evaluation of novel chemical treatment methods for acid sulfate soils. *Science of The Total Environment,* 625**,** 39-49.

Indraratna, B, Medawela S, Rowe RK, Thamwattana N & Heitor A. 2020. Biogeochemical Clogging of Permeable Reactive Barriers in Acid-Sulfate Soil Floodplain. *Journal of Geotechnical and Geoenvironmental Engineering,* 146(5)**,** 04020015. https://doi.org/10.1061/(ASCE)GT.1943-5606.0002231

Indraratna B, Pathirage PU & Banasiak LJ. 2014. Remediation of acidic groundwater by way of permeable reactive barrier. *Environmental Geotechnics*. (*DOI* : https://doi.org/10.1680/envgeo.14.00014)

Indraratna B, Regmi G, Nghiem L & Golab A. 2010. Performance of a PRB for the remediation of acidic groundwater in acid sulfate soil terrain. *Journal Of Geotechnical And Geoenvironmental Engineering, ASCE,* 136**,** 897-906 (*DOI*: https://doi.org/10.1061/(ASCE)GT.1943-5606.0000305)

Johnson R, Blowes D, Robertson W & Jambor J. 2000. The hydrogeochemistry of the Nickel Rim mine tailings impoundment, Sudbury, Ontario. *Journal of Contaminant Hydrology*, 41, 49-80 (*DOI:* https://doi.org/10.1016/S0169-7722(99)00068-6).

Medawela S, Indraratna B , Pathirage U & Heitor A. 2019. Controlling Soil and Water Acidity in Acid Sulfate Soil Terrains Using Permeable Reactive Barriers. *Geotechnics for Transportation Infrastructure.* Springer: 413-426 (DOI: https://link.springer.com/chapter/10.1007/978-981-13-6701-4_27)

Medawela S. & Indraratna B. 2020. Computational modelling to predict the longevity of a permeable reactive barrier in an acidic floodplain. *Computers and Geotechnics,* 124**,** 103605 (DOI: https://doi.org/10.1016/j.compgeo.2020.103605)

Medawela, S.J.M.S.K., 2020. Assessment of Bio-Geochemical Clogging in Permeable Reactive Barriers in Acid Sulphate Soil. Doctor of Philosophy thesis, School of Civil, Mining and Environmental Engineering, University of Wollongong,. https://ro.uow.edu.au/theses1/838 (https://ro.uow.edu.au/theses1/838/)

Medawela S, Indraratna B, Athuraliya S, Lugg G. & Nghiem LD. 2022. Monitoring the performance of permeable reactive barriers constructed in acid sulfate soils. *Engineering Geology***,** 293 (2022): 106465 (DOI: https://doi.org/10.1016/j.enggeo.2021.106465)

Medawela, S., Indraratna, B. and Rowe, R.K., 2023. The reduction in porosity of permeable reactive barriers due to bio-geochemical clogging caused by acidic groundwater flow. *Canadian Geotechnical Journal, (DOI: https://doi.org/10.1139/cgj-2022-0074)*

Monod, J. 1949. The growth of bacterial cultures. *Annual Reviews in Microbiology,* 3**,** 371-394.

NRMMC (National Resource Management Ministerial Council), 2011. Australian Drinking Water Guidelines, National Water Quality Management Strategy, Paper 6. National Health and Medical Research Council, Commonwealth of Australia, Canberra.

Rawlings DE. 2002. Heavy metal mining using microbes 1. *Annual Reviews in Microbiology,* 56**,** 65-91. https://doi.org/10.1146/annurev.micro.56.012302.161052

Shand P, Appleyard S, Simpson SL, Degens B & Mosley, L. 2018. National Acid Sulfate Soils Guidance: Guidance for the dewatering of acid sulfate soils in shallow groundwater environments. Department of Agriculture and Water Resources, Canberra, ACT. CC BY 4.0.

Steefel CI & Lasaga AC. 1994. A coupled model for transport of multiple chemical species and kinetic precipitation/dissolution reactions with application to reactive flow in single phase hydrothermal systems. *American Journal of science,* 294**,** 529-592 (*DOI*: https://doi.org/10.2475/ajs.294.5.529)

INTERNATIONAL SOCIETY FOR
SOIL MECHANICS AND
GEOTECHNICAL ENGINEERING

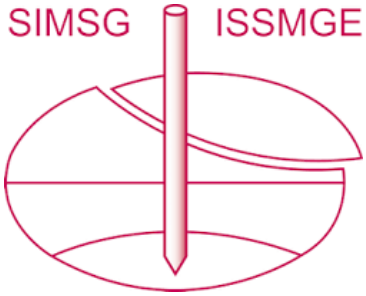

This paper was downloaded from the Online Library of the International Society for Soil Mechanics and Geotechnical Engineering (ISSMGE). The library is available here:

https://www.issmge.org/publications/online-library

This is an open-access database that archives thousands of papers published under the Auspices of the ISSMGE and maintained by the Innovation and Development Committee of ISSMGE.

The paper was published in the proceedings of the 9th International Congress on Environmental Geotechnics (9ICEG), Volume 1, and was edited by Tugce Baser, Arvin Farid, Xunchang Fei and Dimitrios Zekkos. The conference was held from June 25th to June 28th 2023 in Chania, Crete, Greece.